Combination of Geophysical Methods to Support Urban Geological Mapping

A. Gabàs, A. Macau, B. Benjumea, F. Bellmunt, S. Figueras & M. Vilà

Surveys in Geophysics
An International Review Journal
Covering the Entire Field of Geosciences and Related Areas

ISSN 0169-3298
Volume 35
Number 4

Surv Geophys (2014) 35:983-1002
DOI 10.1007/s10712-013-9248-9

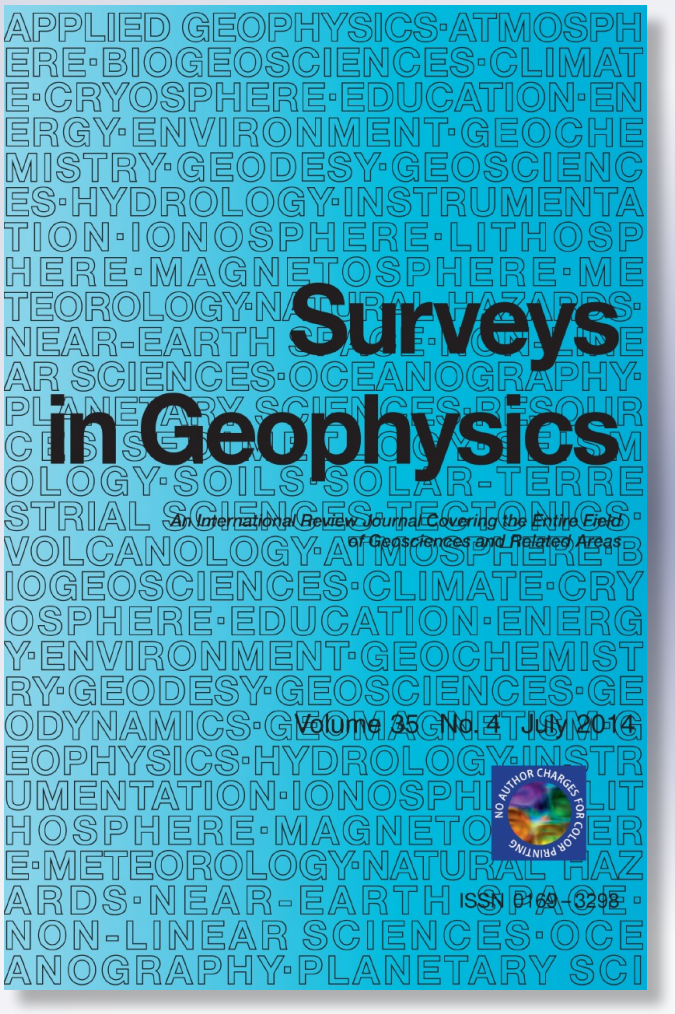

Springer

Surv Geophys (2014) 35:983–1002
DOI 10.1007/s10712-013-9248-9

Combination of Geophysical Methods to Support Urban Geological Mapping

A. Gabàs · A. Macau · B. Benjumea · F. Bellmunt · S. Figueras · M. Vilà

Received: 13 November 2012 / Accepted: 17 July 2013 / Published online: 1 August 2013

Abstract Urban geological mapping is a key to assist management of new developed areas, conversion of current urban areas or assessment of urban geological hazards. Geophysics can have a pivotal role to yield subsurface information in urban areas provided that geophysical methods are capable of dealing with challenges related to these scenarios (e.g., low signal-to-noise ratio or special logistical arrangements). With this principal aim, a specific methodology is developed to characterize lithological changes, to image fault zones and to delineate basin geometry in the urban areas. The process uses the combination of passive and active techniques as complementary data: controlled source audio-magnetotelluric method (CSAMT), magnetotelluric method (MT), microtremor H/V analysis and ambient noise array measurements to overcome the limitations of traditional geophysical methodology. This study is focused in Girona and Salt surrounding areas (NE of Spain) where some uncertainties in subsurface knowledge (maps of bedrock depth and the isopach maps of thickness of quaternary sediments) need to be resolved to carry out the 1:5000 urban geological mapping. These parameters can be estimated using this proposed methodology. (1) Acoustic impedance contrast between Neogene sediments and Paleogene or Paleozoic bedrock is detected with microtremor H/V analysis that provides the soil resonance frequency. The minimum value obtained is 0.4 Hz in Salt city, and the maximum value is the 9.5 Hz in Girona city. The result of this first method is a fast scanner of the geometry of basement. (2) Ambient noise array constrains the bedrock depth using the measurements of shear-wave velocity of soft soil. (3) Finally, the electrical resistivity models contribute with a good description of lithological changes and fault imaging. The conductive materials (1–100 Ωm) are associated with Neogene Basin composed by

Electronic supplementary material The online version of this article (doi:10.1007/s10712-013-9248-9) contains supplementary material, which is available to authorized users.

A. Gabàs (✉) · A. Macau · B. Benjumea · S. Figueras · M. Vilà
Institut Geològic de Catalunya, c/Balmes 209-211, 08006 Barcelona, Spain
e-mail: agabas@igc.cat

F. Bellmunt
Universitat de Barcelona, c/Martí i Franqués s/n, 08028 Barcelona, Spain

unconsolidated detrital sediments; medium resistive materials (100–400 Ωm) correspond to Paleogene, and resistive materials (600–1,000 Ωm) are related with complex basement, granite of Paleozoic. The Neogene basin-basement boundary is constrained between surface and 500 m depth, approximately. The new geophysical methodology presented is an optimized and fast tool to refine geological mapping by adding 2D information to traditional geological data and improving the knowledge of subsoil.

Keywords Audiomagnetotelluric · Microtremor H/V · Ambient noise array · Urban geological mapping · Bedrock depth · Basin geometry · Soft soil—rock interface

1 Introduction

Since 2007, the Institute Geologic de Catalunya (IGC) develops a 1:5000 scale urban geological mapping project which requires detailed subsoil characterization beneath cities and towns of more than 10,000 inhabitants in Catalunya (Spain). The object of this systematic urban geological mapping is to provide a robust database to be used in studies related to urban planning, civil engineering works or environmental studies that society should deal with in the future. The mapping project is integrated in a GIS environment to provide different sets of information, among others: data from previous geotechnical reports, historical, geological and topographic maps, historical aerial photographs, borehole data, geological characterization of outcrops inside the urban and neighboring areas and, finally, geophysical information. All this gathered data is harmonized and stored in a database. The analysis of this database allows to compile and print the 1:5000 scale urban geological map according to the 1:5000 topographic grid of Catalunya (Vilà et al. 2010). The final map is composed of a main geologic map, geological cross sections and complementary maps, charts and tables. One of the most significant complementary maps is the bedrock depth map and the isopach maps of quaternary and anthropogenic deposits.

Geophysical techniques are well suited for obtaining the above mentioned information with two important roles: (1) refining geological mapping by adding 2D and 3D information to 1D borehole data and (2) providing knowledge in areas with scarce subsoil information mainly in zones without boreholes. The combined use of different geophysical techniques is the best way to reduce ambiguities in the estimated subsoil geophysical model. There are a lot of studies and works where is shown the usefulness of combining such different techniques (Gallardo and Meju 2003, 2004, 2007; Kwon et al. 2006; Günther and Rücker 2009; Kim et al. 2007; Falgàs et al. 2011; Grandjean et al. 2011; Colombo et al. 2012). Geophysics is not very effective to uniquely determine lithology, mainly if a single class of geophysical parameters is estimated. This occurs substantially because distinct rock types may be characterized by similar values of one or more geophysical parameters. In general, only the mutual use of different and complementary data sets can be effective in constraining the solution and providing unambiguous geological interpretation at whole range of scales. Hence, the most obvious way to improve the effectiveness of geophysical methods, exploiting their strength and overcoming their weakness is to apply them in combination, jointly determining multiple physical properties (Bosch 1999; Bosch et al. 2002). Within this framework, it was decided to use the combination of different geophysical techniques to support a geological mapping project in an urban

environment with the main goal to overcome the non-uniqueness of the estimated subsoil model.

Considering the urban environment and the scale of this work, we seek a geophysical methodology which is suitable for noisy environments, able to cover large areas and to face restrictions for the deployment of equipment and logistic problems as paved surfaces and roads. The project involves the acquisition of coupled active and passive geophysical data to study subsoil under the cities of Girona and Salt (NE of Spain). The geophysical methods used are (1) Controlled source audiomagnetotellurics (CSAMT), in order to image the near-surface materials and to improve the electromagnetic signal–noise ratio in a particular frequency range with an artificial source, (2) Magnetotelluric method (MT) to study the internal variations of materials as well as faults that control the deep structures. (3) H/V microtremor method to determine the soil fundamental frequency and (4) Ambient noise array measurements to obtain 1D profile shear-wave velocity of the materials of subsoil area. These last both methods are the optimal complementary geophysical data set to determine the thickness of the unconsolidated layer overlying the rigid basement (Meric et al. 2007), avoiding cultural noise and covering large areas with low cost.

Examples of integration of traditional geophysical data for exploration (electric and electromagnetic, seismic, gravity or GPR) can be found largely in the literature. On the contrary, geophysical studies using traditional methods and passive seismic noise are no so common. Dahm et al. (2010) used a combination of different passive geophysical data as microgravity and ambient vibrations to study shallow evaporates beneath urban environment (Hamburg, Germany). Grandjean et al. (2011) applied electrical and seismic 2D imagery methods, passive seismic and EM mapping to characterize the Ballandaz landslide (Savoie, French Alps), and then use this information to provide a combined interpretation of the morpho-structures in order to simulate the geomechanical behavior of the sliding mass. Our own scientific group used the combination of passive seismic noise technique (microtremor H/CV technique) jointly with electrical and seismic 2D tomography to detect the granite bedrock boundary covered by alluvial/colluvial sediments in the Catalan Coast Ranges, NE of Spain (Benjumea et al. 2011a, b). However, we do not know of any work where passive seismic noise is combined with magnetotelluric method.

The aim of the present study is to assess the potential of the developed methodology (combination of magnetotelluric and passive seismic noise techniques) to recognize and characterize lithologies and structures of subsoil in heavily build-up areas, where large-scale geophysical experiments are often difficult, if not impossible. The results show the advantages and limitations of the proposed methodology created as a suitable and fast tool for the systematic development of 1:5000 urban geological mapping projects.

1.1 Geological Setting and Survey Area

The study area is located in NE of Spain and includes the cities of Girona and Salt (Fig. 1). This area is within the northern part of the "La Selva" basin, integrated in a range and basin tectonic area created during the distensive periods following the Alpine orogeny during the Neogene. The tectonic and morphological evolution of the basin was determined by two main fault directions, NW-SE and NE-SW (Donville 1976; Saula et al. 1994). The basin sedimentary infill consists of Neogene and Quaternary sediments derived from the erosion of the surrounding reliefs. The basin boundaries were affected also by volcanic episodes. A brief description of the most representative units in the study area is presented in Fig. 2.

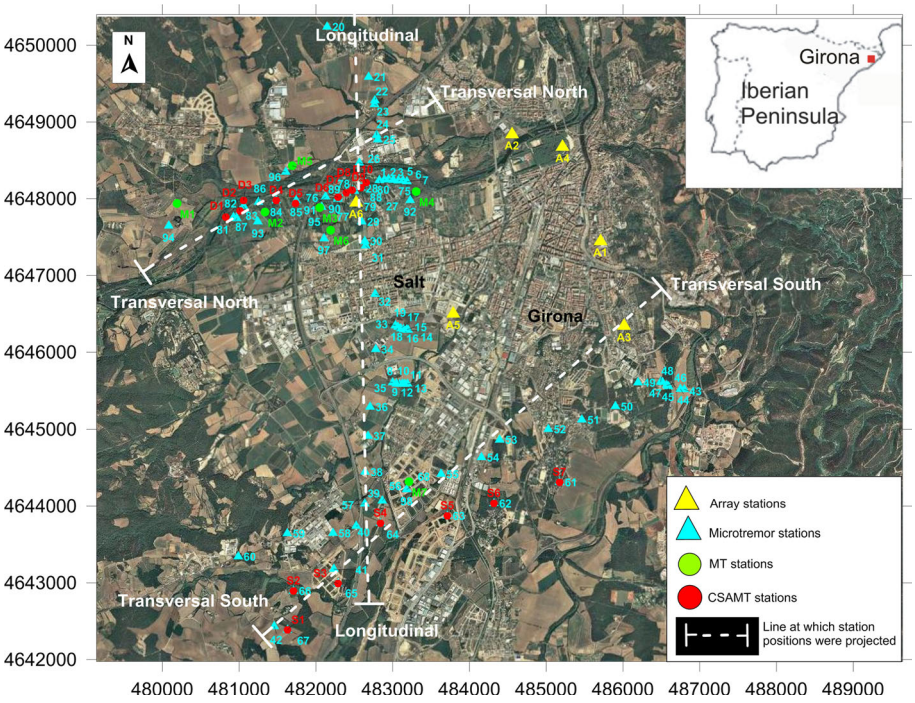

Fig. 1 Map of survey *lines* for surface geophysical methods performed at the surroundings of the Salt and Girona cities. UTM coordinates ED50 Zone 31 N. Sites are represented by triangles (*yellow sites* have array data and *blue sites* have microtremor data) and *circles* (*green sites* have MT data and *red sites* have CSAMT data)

The Paleozoic igneous and metamorphic rocks and the Paleogene sedimentary rocks are the lithologies of the "La Selva" basin surrounding range areas (Littoral and Prelitoral coastal ranges and Transversal mountain range, respectively), which constitute also the basin basement. The Paleogene sediments are represented by the Paleocen-Eocene Pontils Group (Ferrer 1971), which consists of detrital facies fluvio-alluvial and Eocene limestones (Pallí 1972) with abundant miliolidae, alveoline and remains of molluscs in the lower part and foraminifera of the genus Nummulites in the upper part.

The Neogene unconsolidated detrital sediments (alluvial fan systems) constitute the main infill of the "La Selva" basin. In the study area, their outcrops are mainly restricted to the south of Girona, because they are covered by quaternary sediments near Salt city. Because of its low fossil content, it is difficult to discriminate between Miocene or Pliocene ages. In the area near Salt city, where Neogene materials can be attributed to Pliocene age (Solé 1948), the thickness of this unit is quite variable, reaching 50–100 m thickness on average. However, they can reach up to 250 m depth depending on the structure of the basin floor.

The quaternary deposits cover much of the studied area and are mainly composed by detrital deposits with a range between (1 and 20 m). The volcanic materials outcrop to the north of the study area and consist of basanites (Pleistocene age), which constitute the upper terminal part of the Puig d'Adri volcanic flow. Its maximum thickness is about 25 m.

Figure 3 presents a cross section showing the subsurface geological structure of the study area that was inferred from the 1:25000 geological map information (332 2–1 Salt;

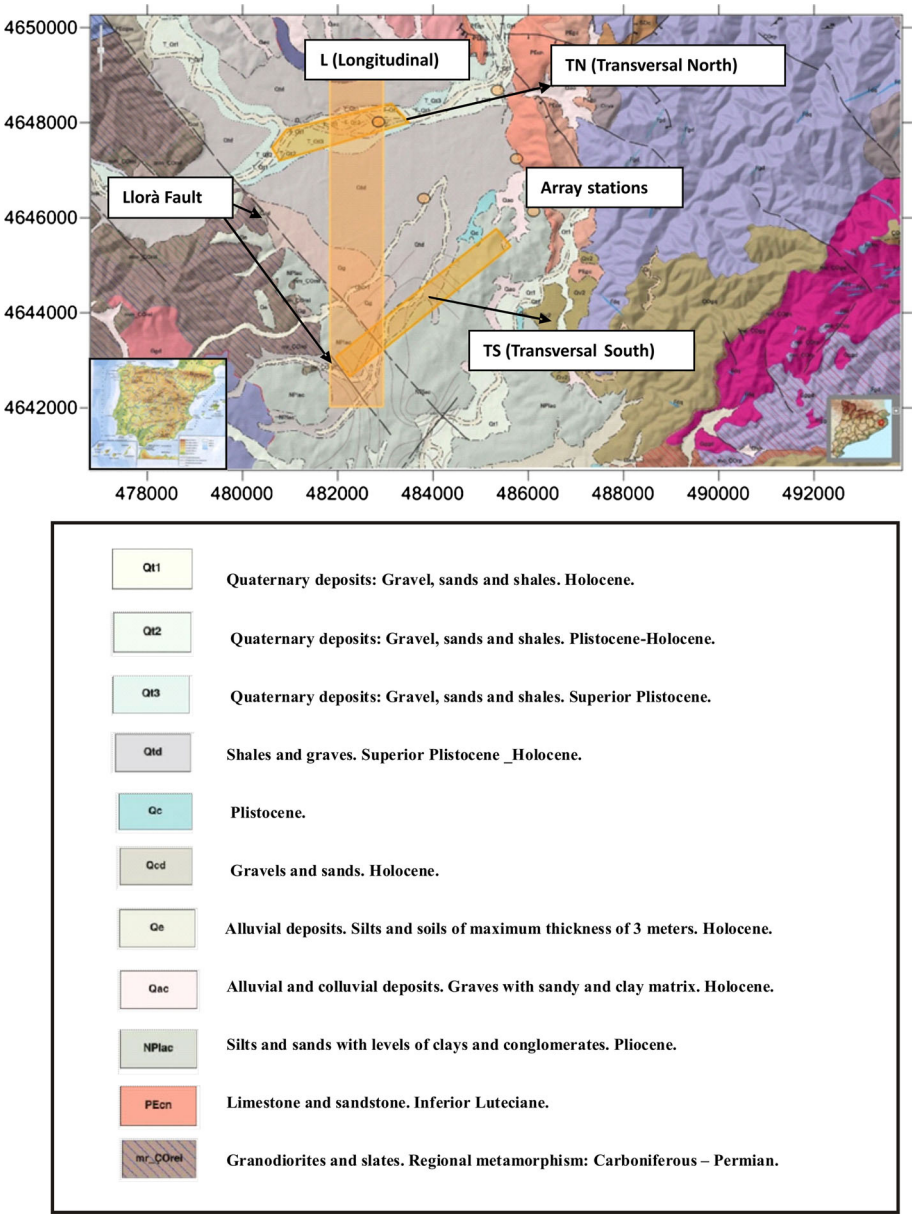

Fig. 2 Map showing the main geological features derived from geological map 1:50000 in the studied area. *Orange rectangles* show the location of the CSAMT, MT, H/V surveys, and *orange circles* show ambient noise array stations in the surroundings of Salt and Girona cities (TN, Transversal North; TS, Transversal South and L, Longitudinal profiles)

IGC 2003–2009) previously to the present work. The applied geophysical techniques will be used to support, improve or refute the outcrop-based information, e.g., to establish accurately the depth of the basin basement, thickness of the infill geological units or the location of buried faults (Llorà and Cartellà faults).

2 Methodology

Within the course of this project, an important amount of new multi-geophysics data was acquired using four geophysical techniques (CSAMT, MT, H/V and seismic noise array). Each method presents its benefits and sensitivity which are exploited by the developed methodology. These methods are sensitive to structure, lithology, fracture, geometry of bedrock depth and mechanical properties of soils, always at a regional scale, first 1,000 m of subsoil.

The main steps of the methodology presented in this work are summarized as follows:

- First step: H/V microtremor technique (Nogoshi and Igarashi 1971; Nakamura 1989; Bard 1985; Fäh et al. 2001) was applied as an efficient way of obtaining soil fundamental frequency ($f_{H/V}$) in the study area. This value ($f_{H/V}$) is the lowest frequency corresponding to a spectral H/V peak, and it is related to a strong impedance contrast, usually soil–rock interface. Three different topologies of the H/V ratio have been obtained to interpret the depth of the soil-rock in contact (Fig. 4). Measurements over shallow bedrock are characterized by a clear peak at high frequencies (above 1 Hz) (Fig. 4a). Deep bedrock sites show a spectral peak at lower frequencies (below 1 Hz) (Fig. 4b). Finally, stations located over bedrock are characterized by the lack of a clear maximum in the curve with amplitudes lower than two over the whole frequency range (Fig. 4c). As an exploration tool, H/V microtremor technique is a way of obtaining an estimation of soil-rock boundary geometry (Ibs-von Seht and Wohlenberg 1999; Delgado et al. 2000a; Parolai et al. 2002; Benjumea et al. 2011a, b). Therefore, it

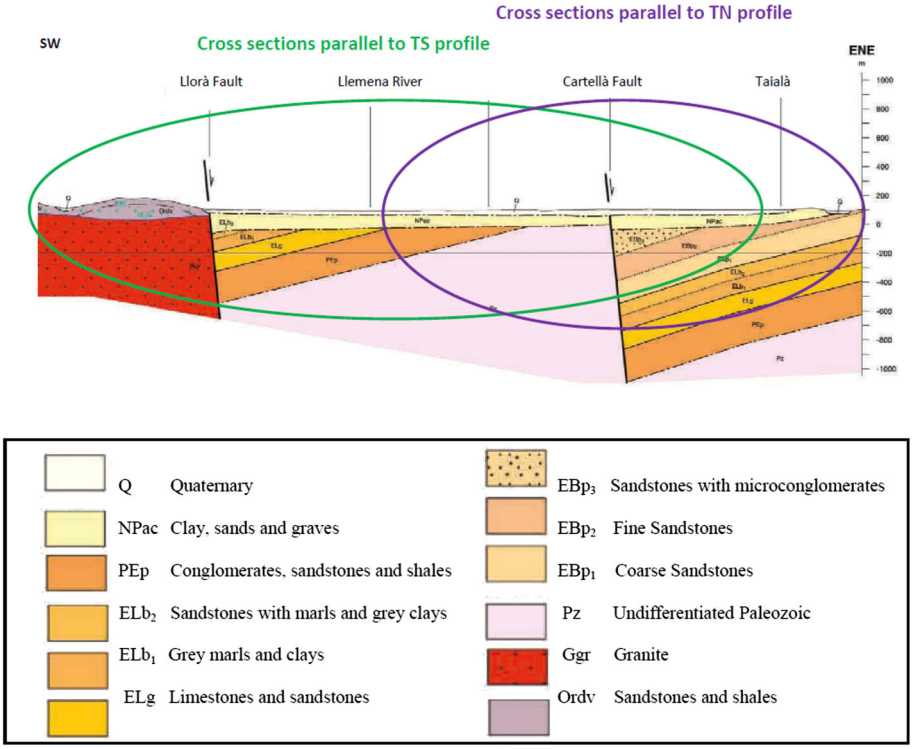

Fig. 3 Geological cross section of 1:25000 scale geological mapping, 332 2–1, Salt (IGC 2003–2009)

presents some limitations that are presented by Delgado et al. (2000b) and Guéguen et al. (2007). They described the factors that can increase the error in bedrock depth estimation when valleys with a strong 2D or 3D structure are studied.

- Second step: H/V peaks are directly transformed to pseudo-depth (H) by means of an empirical relation, which was estimated by linear regression at points where borehole stratigraphies or shear-wave velocity profiles from dispersion curve inversion were available (Kühn et al. 2010). Passive geophysical methods (microtremor array data) were applied as cost-effective method to obtain time-average shear-wave velocity V_{sz} from surface to z meters depth (Asten and Henstridge 1984; Aki 1957; Bard 1985) and soil fundamental frequency (Macau et al. 2012). The pair of values (V_s, H) is obtained from dispersion curve inversion, and $f_{H/V}$ is calculated according to expression (1) (Bard 1985):

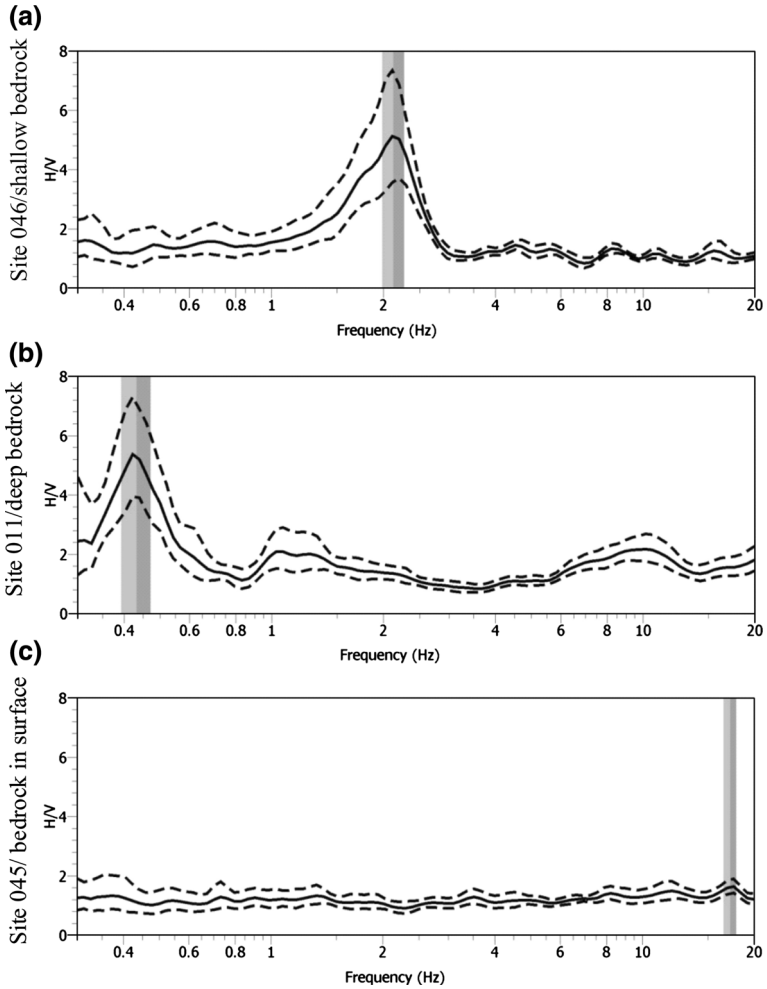

Fig. 4 Topology of the H/V curves observed in the study area: shallow bedrock site (**a**), deep bedrock site (**b**) and rock site (**c**). *Black solid lines* and *dashed lines* indicate the average spectral ratio and the corresponding standard deviation. Vertical *gray bars* identify the soil fundamental frequencies and their errors

$$f_{H/V} = \frac{V_s}{4H} \quad (1)$$

Cadet et al. (2011) checked the coherence of this estimated value from ambient noise array compared with SPT-V_s empirical correlations.

- Third step: the empirical relationships described by other authors in the step 1 (Ibs-von Seht and Wohlenberg 1999; Delgado et al. 2000a; Parolai et al. 2002; Benjumea et al. 2011a, b) are represented in lineal space jointly with the pair ($f_{H/V}$, H) of the second step (array and H/V data). The comparison between both values allows us to choose the empirical expression that better fits to Salt and Girona data (Fig. 5) to interpolate pseudo-depth (H) with the aim of obtaining a 2D geometry profile of the bedrock depth (2):

$$H = a.f_{H/V}^{b} \quad (2)$$

H is the overburden thickness in meters, $f_{H/V}$ is the soil fundamental frequency, and a and b are empirical parameters which values depend on the chosen expression.

- Fourth step: use of 2D magnetotelluric and controlled source audiomagnetotelluric data to obtain an electrical resistivity model of the subsurface. With this model, we can obtain information about local near-surface sediments characterization, deep bedrock and location of faults and fractures.
- Fifth step: correlation of all geophysical models and previous known geological information. The result obtained from passive seismic noise (bedrock geometry) is used as a constrain and is correlated with electrical resistivity models (CSAMT and MT) in order to obtain a high coherence in the final interpretation.

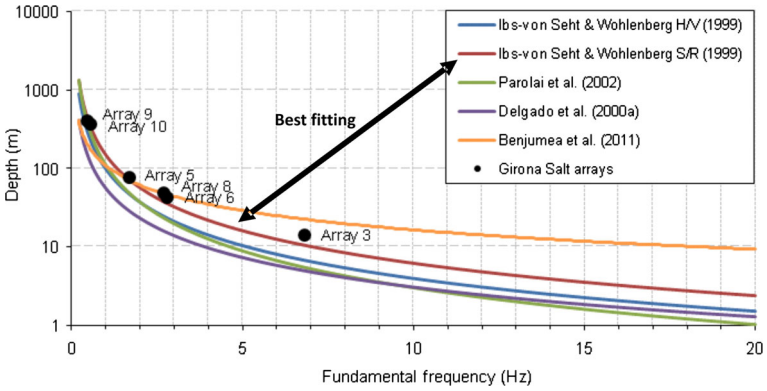

Fig. 5 Comparison between sediment thickness from ambient noise array carried out in Girona and Salt cities (6 black points) and bedrock depth curves obtained using empirical expressions calculated by other authors in other studied regions

2.1 Data Acquisition and Processing

2.1.1 Microtremor H/V Measurements

During 2010, a total of 87 seismic noise stations were distributed along three profiles to delineate the geometry of the bedrock in different directions, W-E (Transversal North and Transversal South profiles) and N–S (Longitudinal profile). Transversal North and Transversal South profiles are coincident with electromagnetic data while the longitudinal profile is acquired only with the microtremor technique, since it crosses the densely populated area of Salt from North to South (Fig. 1).

This method consists of estimating the ratio between the Fourier amplitude spectra of the horizontal and the vertical components of seismic noise vibrations. It is generally accepted that this spectra provides a good estimation of the fundamental frequency of soft soil ($f_{H/V}$) following the guidelines of the SESAME (Site Effects Assessment using Amient Excitations) project (Bard and SESAME-Team 2004). One of the requirements in applying H/V method to calculate soil fundamental frequency is that there must exist a sharp acoustic impedance (>2) contrast between sediments and underlying rock (Lachet and Bard 1994; Konno and Ohmachi 1998; Fäh et al. 2001; Bonnefoy-Claudet 2004).

The microtremor data were recorded using a six-channel Cityshark datalogger connected to two Lennartz 0.2 Hz LE-3-D three-component sensors. Record length ranged between 10 and 20 min with a sampling frequency of 100 Hz. The microtremor H/V curves were calculated using the Geopsy software (http://www.geopsy.org), as indicated in this expression:

$$\frac{\mathrm{H}}{\mathrm{V}} = \frac{S_{NS} + S_{EW}}{2.S_V} \tag{3}$$

where S_{NS}, S_{EW} and S_V are the magnitudes of the spectrum Fourier method of north–south, east–west and vertical components, respectively. The Fourier spectrum for each component was smoothed in overlapped windows by 50 %. Sectors with non-stationary signal have been removed applying a STA/LTA anti-trigger algorithm (Lee and Stewart 1981).

2.1.2 Ambient Noise Array Measurements

As part of a microzonation project carried out in the city of Girona from 2009 to 2011, 10 sites were investigated with the array technique (Macau 2012). From these data sets, only six arrays measurements were used in this work as can be seen in Fig. 1.

Two different equipments were used for array data acquisition. The array configuration consists of one sensor at the center and five sensors arranged in various concentric circles with different radius, increasing from 25 to 500 m in function of investigation depth. Subsequently, record length was increased up to 60 min for the largest aperture array with a sample interval of 5 ms.

For shallow bedrock, the equipment was composed of eleven 1 Hz Mark Products L-4 sensors connected to DMT summit acquisition system distributed in two circles (25 and 50 m radius) with a common center station. In this configuration the maximum investigation depth was 100 m and the record length was 30 min (arrays A1-A5).

For a large-scale study, 6 Lennartz 5 s three components seismometers have been used with 6 SARA S06 datalogger. The maximum investigation depth was 1,000 m and the record length was 60 min (array A6).

Data processing for obtaining shear-wave profile is divided into two main steps: deriving a spectral curve characteristic of the propagating waves (dispersion curve or autocorrelation curves), and inverting this curve to retrieve the soil structure (Wathelet et al. 2008). These data were analyzed with the frequency-wave number (FK) and spatial autocorrelation (SPAC) methods (Aki 1957) and the inversion processing (dispersion curve from FK and SPAC) has been done with the Dinver software included in the GEOPSY package (http://www.geopsy.org) based on a neighborhood algorithm (Wathelet 2003; Wathelet et al. 2004). This process follows the guidelines proposed by SESAME research group (http://SESAME-FP5.obs.ujf-grenoble.fr).

2.1.3 Electromagnetic Methods (CSAMT, MT)

Within the family of electromagnetic methods, controlled source audio-magnetotelluric method, CSAMT, and the magnetotelluric method, MT, involve measuring the temporal fluctuations of the horizontal and vertical components of the natural electromagnetic field at the Earth's surface. These fluctuations are caused by the ionosphere related with solar activity in the low frequency range, and the world wide thunderstorm activity at higher frequencies. Both passive (MT) and active (CSAMT) electromagnetic methods provide the electrical resistivity of the earth's crust for different depth ranges.

The CSAMT and the MT surveys carried out during 2010 consisted of 21 stations along two electromagnetic profiles: Transversal North (TN) and Transversal South (TS) (Fig. 1). The total lengths of the profiles were about 3 km (TN) and 4 km (TS) and, on average, the distance between the stations with CSAMT or MT data was about 400 m.

In this study two different instrumentations were used to perform the electromagnetic measurements. Geometrics Stratagem EH4 system is used in the high frequency range (low periods) for CSAMT measurements (17 sites, red circles in Fig. 1) and it is generally applied for mapping the first 500 m of the subsurface (Zonge and Hugues 1991). In the CSAMT method, an artificial electromagnetic signal is used to obtain a continuous electrical sounding of Earth beneath the measurement site (Geometrics 2000) in a frequency range from 10 to 92,000 Hz. The natural signals are typically weak in the frequency range from 1,000 to 64,000 Hz and an unpolarized transmitter was used to improve signal-to-noise ratio and to minimize the effect of cultural noise and improve the data quality. In the study area, that transmitter was located around 100 m from the recording system, far enough away to accomplish the plane wave hypothesis, but close enough to see the transmitter signal (Falgàs et al. 2011).

ADU07 (Metronix) system is used in order to cover the low frequency range (long period) and to investigate deep structures for MT measurements. The MT technique has proven useful in a broad range of frequencies (128 to 4,096 Hz) with target depths higher than 1 km. Seven MT sites were acquired but only four of them were used to invert data due to noise effects.

Combinations of both techniques are essential for assuring high-resolution imaging of near-surface and suitable depth range for large-scale studies [estimating lateral and vertical variations of electrical conductivity of the Earth's interior (Vozoff 1991)] and indicated for geological investigation given the sensitivity of electrical resistivity to the presence of different lithologies. Keep in mind that the electrical resistivity parameter is largely dependent upon their fluid content, porosity, degree of fracturing, temperature and conductive mineral content (Keller 1987). Tables of electrical resistivity of a variety of rocks, minerals and geological environments may be found in Keller (1987) and Palacky (1987).

Due to urban conditions, the acquired time series data suffer low signal-to-noise ratio in the high frequency range. Thus, careful data processing was performed and corrupted segments in the time series data were removed. The impedance tensor response, parameterized as apparent resistivity and phase, are obtained from the time series signals. The magnetotelluric processing follows a traditional analysis. First, in order to determine the dimensionality of the regional structures and to obtain the regional impedance tensor, we applied the Groom and Bailey (1989) method following the scheme of McNeice and Jones (2001). Geoelectric strike directions of individual sites were estimated from the MT impedance tensor at each site for all the frequencies with an error floor of 5 % on the impedance tensor components. The best-fit average multi-site, multi-frequency regional strike was N35°W for the frequency band between 1.5×10^{-5} and 1.5 Hz, which is consistent with the strike of the main surface geological structure determined as N40°W. The individual site estimates of strike are weighted by the error misfit. Misfit values with RMS less than 2.0 are considered reliable, whereas larger misfits are indicative of three-dimensional effects (Ledo et al. 2011). In this study, only one site is greater than threshold 2.0, the other sites display a RMS value less than 2.0 indicating the behavior of the structure according to two-dimensional (Fig. 6). Second, the static shift effect was corrected using three electrical resistivity models obtained during 2009 shallow geophysical survey (Benjumea et al. 2011a, b), taking an average value of 100 Ωm for the first 50 m in the TE and TM modes for CSAMT data.

2D electrical resistivity models have been constructed inverting simultaneously the TE and TM mode of the apparent resistivity and phase, with the algorithm of RLM2DI (Rodi and Mackie 2001). This algorithm searches the lowest overall RMS misfit with the smallest lateral and vertical conductivity gradients in a regularized manner, following the approach pioneered for MT data by Constable et al. (1987). In the inversion process, we used a 100 Ωm half space as the initial model and neither structural feature nor conductivity

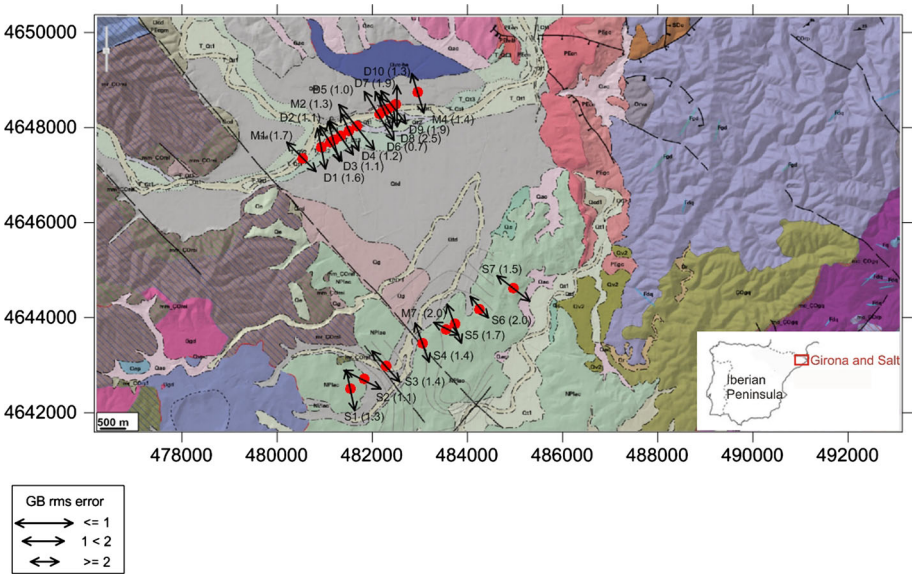

Fig. 6 Location of the CSAMT and MT stations (*red spots*) in a Geological map of the study area. The *arrows* indicate the strike direction of each site for all frequencies and their lengths are associated with the compatibility of the data to assume two-dimensional data in the suggested strike direction

discontinuities were imposed. An error floor of 10 % for the apparent resistivity and 2.86° for the phases has been used for the inversion process giving equal weight to all data type (Gabàs and Marcuello 2003). The final models were obtained using smooth curves with 10 % D + values (Beamish and Travassos 1992). This type of smoothing forces the curves to have coherence between apparent resistivity and phases (Campanyà et al. 2012). Figures A1 and A2 shows the calculated curves superimposed on the raw data. The smooth curves have been used in the two-dimensional inversion process to avoid unnecessary structures as much as possible and fill the gap in sites where some frequencies with low natural signal or high electromagnetic noise.

The last process to accept the final models is the resolution analysis of the geoelectrical model using the sensitivity test. This test consists on comparing the differences between final models and modified models, where some properties of the studied features have been changed (geometry of the structures or their electrical resistivity). If the modified model provides an increase in the RMS of some sites, it can be understand that the modification is excluded, and as a consequence, the structure or feature of the initial model is necessary to explain the data raw. Conversely, if the RMS value is lower than the RMS initial value, we assume that the data have no enough resolution to constrain that structure.

3 Results

In the following section, we, respectively, analyze the contribution of passive seismic noise (H/V and array technique) and electromagnetic data (CSAMT and MT). The combined interpretation of the result derived from these various methods is then discussed.

3.1 Passive Seismic Noise (H/V and array)

We obtained the overburden thickness (H) using the soil fundamental frequency ($f_{H/V}$) of microtremor H/V technique at each site along TN, TS and L profiles, and the empirical relationship of Ibs-Von Seht and Wolhenberg S/R (1999). This expression shows the best fit to the array results as can be observed in Fig. 5, and it is described as

$$H = 146.\left(f_{\frac{H}{V}}\right)^{-1.375} \tag{4}$$

The results of these bedrock topographies (sediment thickness) are shown in Fig. 7 and can be summarized in each profile as follows:

- **TN profile**: The minimum soil fundamental frequency is 0.4 Hz (red circles at Fig. 7) in center of the profile, in Salt city. This implies a maximum thickness of soft sediments about 515 m. Similar $f_{H/V}$, corresponding to constant and high bedrock depth values, are observed at the remaining of the stations.
- **TS profile**: Very shallow bedrock is detected at the ends of the profile (lack of peak in the H/V ratio). Basement outcrops are observed at both East and West sides (purple circles at Fig. 7). In the center of profile, the soil fundamental frequency is about 0.5 Hz, corresponding to 400 m of bedrock depth (yellow circles).
- **L profile**: A decrease in the soft sediment thickness is observed at both ends of the profile (blue circles in Fig. 7), with a minimum value about 120 m. However, bedrock outcrops are not observed in the vicinities.

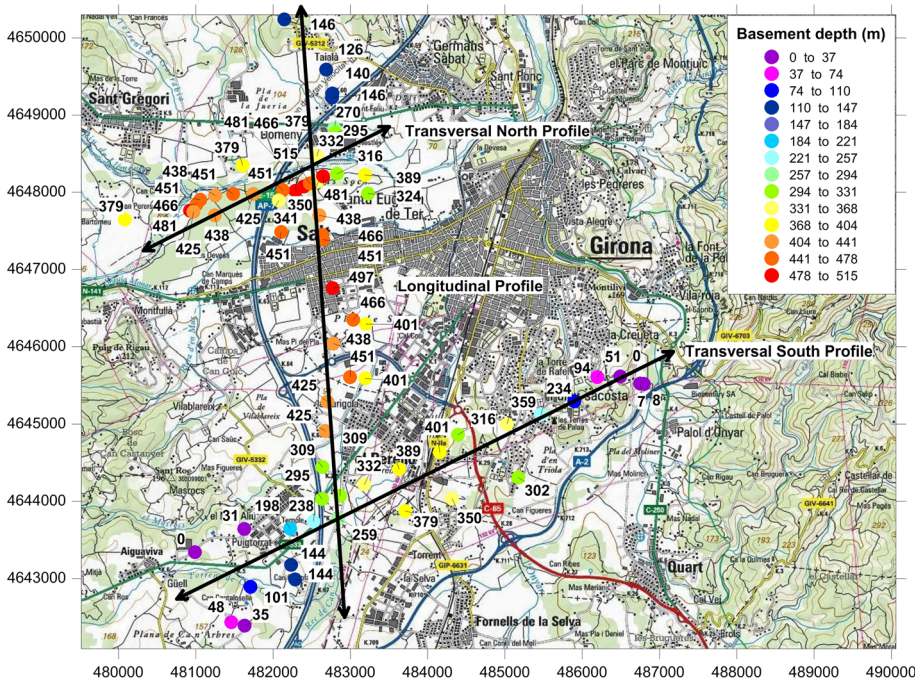

Fig. 7 Overburden thickness of Neogene materials calculated from soil fundamental frequency using the relationship proposed by Ibs-von Seht and Wohlenberg S/R (1999)

Using the combination of H/V spectral microtremor and ambient noise array measurements, it is possible to define the depth of soft soil—rock interface along these three profiles because there is an important contrast in their impedance properties, but other exploration methods are necessary to identify lithologies.

3.1.1 Electromagnetic Techniques (CSAMT and MT)

The obtained resistivity models are shown in Figs. 8 and 9. Comparing modes TE and TM of both profiles (TN and TS), the TM mode provided a better fit between the model response and the acquired data in both profiles of the study area. In spite of this, the inversion procedure was carried out using data of both modes in order to obtain the most realistic result using all information. The misfit between the data and the model responses has an RMS value of 5, approximately. This is a remarkably good level of fit achieved in the vicinity of urban areas. The geoelectrical images reveal the location of a high resistivity zone (500–1,000 Ωm) at lower frequencies that could be associated with the presence of the basement. In contrast, at higher frequencies, a low resistivity area (30 Ωm) shows the sedimentary material of the basin jointly with some resistive shallow bodies (500 Ωm). The residuals between the observed data and the model responses are shown in the Figs. 10 and 11 for both profiles TN and TS, respectively. The values are acceptable, and no strong feature in the data is unexplained. However, due to low quality of some measurements for low frequencies, some data were not included in the inversion procedure. According to this, considering the range of measured electrical resistivity values (30–1,000 Ωm) and the known skin depth relationship, the final skin depth is variable along two profiles, and the

final electrical models are characterized by a high sensitivity up to 800 or 1,000 m. Finally, raw data and response data are compared in the figures of appendix, figures A1-1, A1-2, A1-3 and A2-1, A2-2, with corresponding RMS for each survey.

In order to know the resolution of the CSAMT-MT final models and to justify the presence of the main geoelectrical structures (resistive bodies and basement), a nonlinear sensitivity test was carried out. The test basically consists to remove some basement structures changing their electrical resistivity values (>1,000 Ω·m) by the neighbor's electrical resistivity values (100 Ω·m). In the TN profile, the changes were focused in the elimination of the two shallow resistive bodies located in the Neogen Basin. In the TS profile, the changes were focused in the Paleozoic basement (granite). In all cases, it is observed a recovery of similar resistive structures in the final inversion model. Also, a significant increase in the RMS value in some sites suggests that the structures here analyzed are necessary to explain the raw data. The obtained constraints show a range between 1,000 and 5,000 Ω·m in both profiles (TN and TS) for the resistive bodies and a variation between 50 and 100 m depth for the upper boundary of these features.

3.2 Joint Interpretation

The combined interpretation of the passive seismic noise (H/V and array) and the electromagnetic (CSAMT and MT) results from these profiles help improve the interpretation of the subsoil structure imaging. In order to interpret which geological contact is detected by H/V peak frequencies, the geoelectrical model and calculated depth values from H/V technique have been superimposed (Figs. 8, 9). The impedance contrast between overburden (Neogene) and basement (Paleogene or Paleozoic) has been considered as the cause of the soil resonance since these materials present an important change in its mechanical properties (e.g., V_s).

In general, the geoelectrical models indicate a near-surface conducting layer with a resistive basement at variable depth, from 100 to 500 m, approximately. The electrical resistivity models exhibit three different zones: A wide and low resistive zone

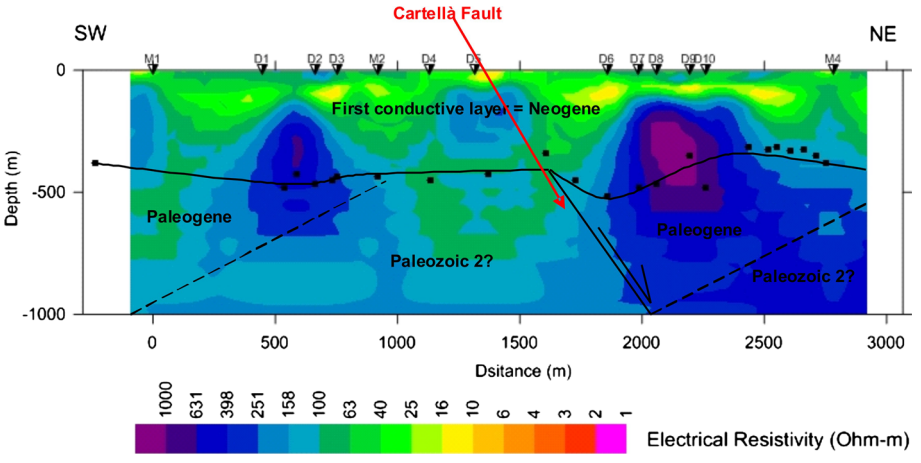

Fig. 8 Two-dimensional CSAMT and MT resistivity model along the Transversal North survey *line*. *Black dots* mark bedrock depth obtained from $f_{H/V}$-depth empirical relationship (Ibs-Von Seht and Wolhenberg S/R, 1999)

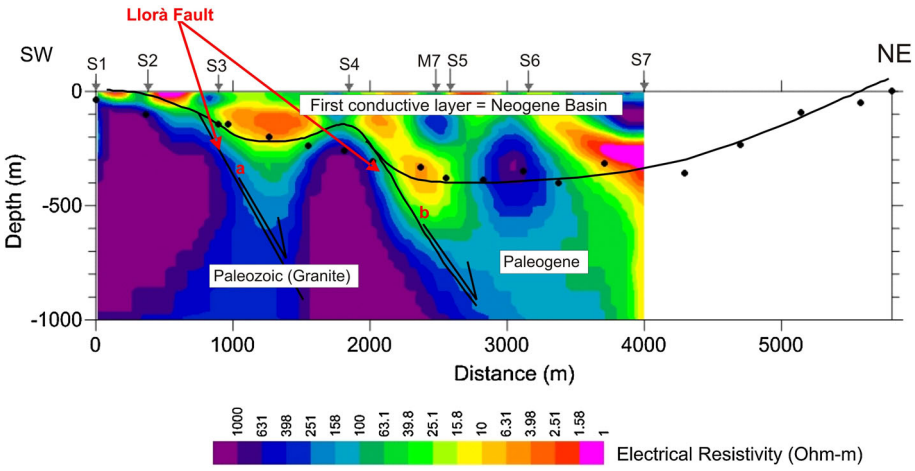

Fig. 9 Two-dimensional CSAMT and MT resistivity model along the Transversal South survey line. *Black dots* mark bedrock depth obtained from $f_{H/V}$-depth empirical relationship (Ibs-Von Seht and Wolhenberg S/R, 1999)

(1–100 Ω·m) noted as **first conductive layer**, which is shown in both profiles with a variable depth from surface at the western part of the models up to a maximum of 500 m at the middle and eastern part of the profile. This zone has been interpreted as sedimentary materials of **Neogene Basin** (clay, sands and gravel levels). Some isolated resistive bodies (400–600 Ω·m) can be observed within this first conductive layer interpreted as gravel and sand bodies. The maximum depth of this first conductive layer is 450 m, approximately. **The second zone** is characterized by medium resistivity values ranging between 100 and 400 Ω·m and can be located in different parts of the model at a depth of 500 m, approximately. This middle resistive area would correspond to **Paleogene materials** consisting of sandstones, marls, conglomerates and lutites. In the TN profile, this second layer fills the whole model in a smooth contrast with the other lithologies, while in the TS profile, the Paleogene material is located only in the eastern part of the model. Finally, in the TS profile, an important third deeper layer has been detected. This layer is characterized by most resistive materials (600-1,000 Ω·m) that may be related with **Paleozoic bedrock** (granite). This basement is detected close to surface (100 m) in the western part of model (site S1), at 200 m depth in the middle of the model (site S4) and reaches the 1,000 m depth at the end of model (between sites M7 and S5). This profile crosses the Llorà fault (Fig. 3) which could be detected as a fault system in the geoelectrical image of Fig. 9, over sites S3 and S4.

Regarding H/V measurements, the obtained sediment/basement interface is in good agreement with the geoelectrical model (black dots at Figs. 8, 9). The soil–rock contact depth coming from H/V peak is detected between 100 and 500 m depth in both profiles. It can be observed that this bedrock is related to two different types of lithologies according to the geoelectrical models (Figs. 8, 9). In the western part of TS model, the contact between Neogene and Paleozoic (granite) materials is interpreted as the main impedance contrast mapped using H/V technique. This contact coincides with an important contrast in the resistivity model. A different behavior is shown in the eastern part of TS and in whole TN model where the main impedance contrast is given between Neogene and Paleogene materials. This change of material is more diffuse from a geoelectrical viewpoint. For this

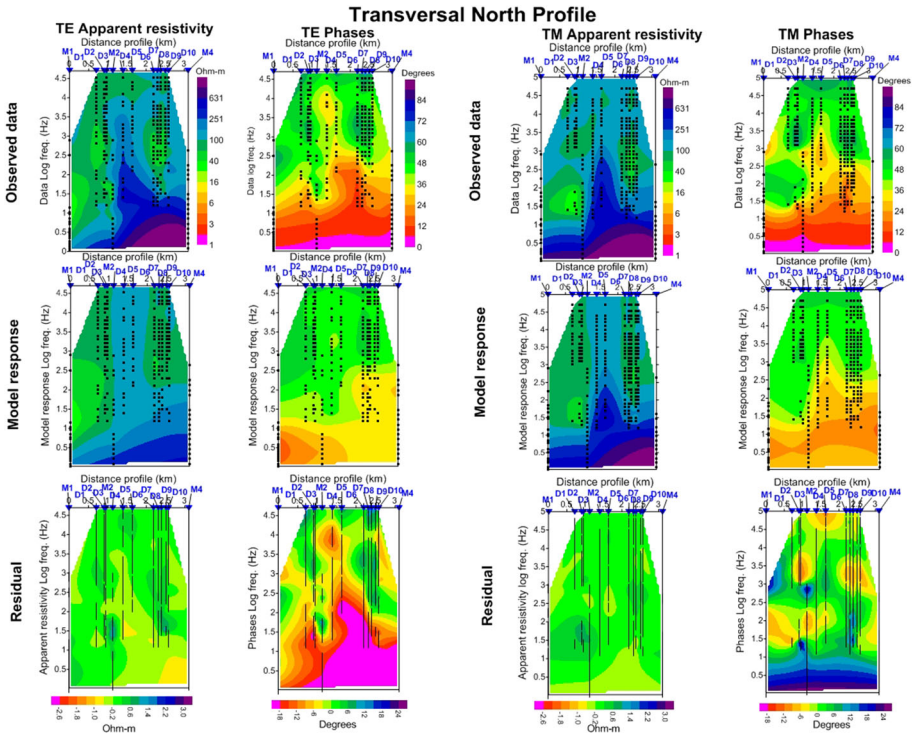

Fig. 10 Comparison between the TN observed data (*top*) and the TN model responses (*middle*) for TE and TM modes (*left* and *right* site, respectively). At the *bottom*, the pseudosection of the residuals for the apparent resistivity (Model responses minus raw data divided by raw data). The same images are presented for the phases. At the *top*, observed data of the phase, at the middle model response of the phase and at the *bottom* the residual of phase (Model responses minus raw data). Tiny *black dots* are smooth data points used for the inversion. *Black lines* in the residual pseudosection show the range of frequencies used for each site for the inversion. Sites are represented by blue inverted triangles (CSAMT and MT data). The misfit between data and the model responses has a RMS value of 4.5

reason, in this geological framework, the use of H/V measurements is a useful geophysical tool to delineate the base of Neogene since it allows constraining the CSAMT and MT interpretation as well as extending basement delineation in noisy urban areas.

4 Conclusions

We collected and compiled different types of geophysical data to develop a useful methodology to improve an urban geological mapping under noisy conditions. The final models provide a more accurate knowledge of the structures around Girona and Salt cities than using only one geophysical technique or only geological information. A special methodical focus is the comparison between all applied techniques, exploiting their advantages and avoiding their limitations. Complementary techniques are chosen; the restrictions of one technique are solved with the other one using a reciprocal exchange between them.

We can conclude that

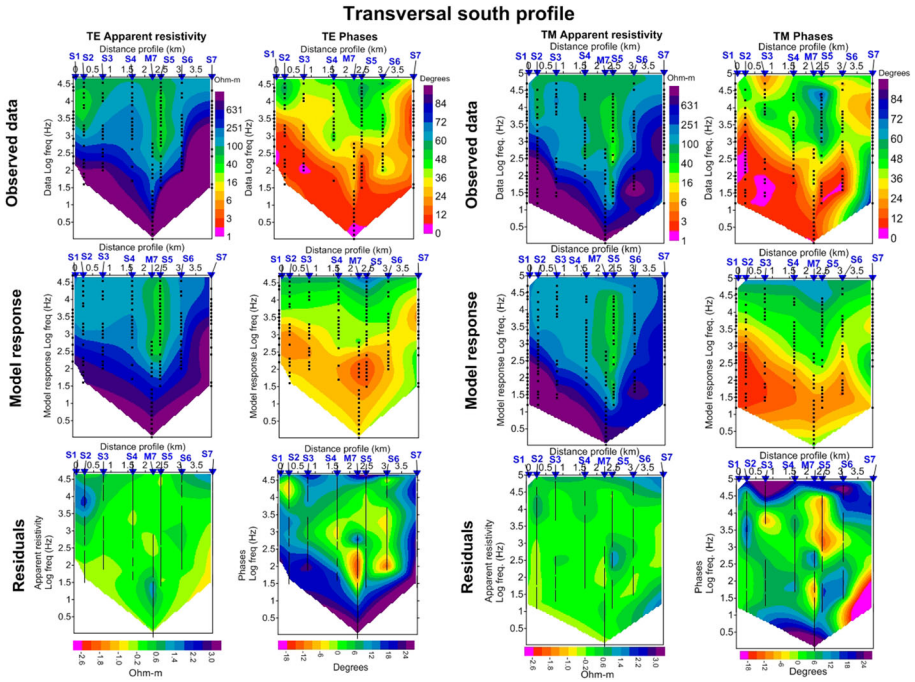

Fig. 11 Comparison between the TS observed data (*top*) and the TS model responses (*middle*) for TE and TM modes (*left* and *right* site, respectively). At the *bottom*, the pseudosection of the residuals for the apparent resistivity (Model responses minus raw data divided by raw data). The same images are presented for the phases. At the *top*, observed data of the phase, at the middle model response of the phase and at the *bottom* the residual of phase (Model responses minus raw data). Tiny *black dots* are smooth data points used for the inversion. *Black lines* in the residual pseudosection show the range of frequencies used for each site for the inversion. Sites are represented by *blue* inverted *triangles* (CSAMT and MT data). The misfit between data and the model responses has a RMS value of 5.1

- The combination of H/V measurements and ambient noise array offers an efficient tool to know the bedrock depth and delineate the geometry in extended areas. But, with these techniques, it is not possible to define which lithologies compose the overburden and basement of subsoil. Hence, a complementary method is necessary.
- We propose to apply the CSAMT/MT techniques which provide a good image of subsoil taking into account the geoelectrical behavior of the materials. The electrical resistivity parameter distinguishes between lithologies and locates the buried faults. But, it is necessary that a significant contrast in this parameter to identify materials with an adequate resolution. If this is not the case, passive seismic noise data could overcome this limitation.
- CSAMT and MT methods present poor quality data in highly urbanized areas due to noise effect. For this reason, the geophysical investigations are applied outside the cities with the purpose of infer, later, this new acquired knowledge inside the downtown area with the support of passive seismic noise.

The synergy between physical properties is the future of geophysical studies to overcome the non-uniqueness of models. In this study, the joint interpretation of geological information, CSAMT, MT profiles, H/V surveys and ambient noise array measurements

provide more insights and reduce uncertainties of subsurface model. As a consequence, these results improve significantly the knowledge used in the development of the urban geological mapping. The developed methodology is successfully applied in other urban geological mapping of Catalunya.

Acknowledgments All of the authors would like to acknowledge all the persons helping during the stages of data acquisition and processing. We also thank Dr. J. Ledo for his suggestions and help to improve this paper. This fieldwork was part of microzonation project developed in Girona city during 2009–2010 and 2011 within the framework of SISPYR project (Seismic information system for the Pyrenees, INTERREG IV-A-2007-2013).

References

Aki K (1957) Space and time spectra of stationary stochastic waves, with special reference to microtremors. Bull Earthq Res Inst 22:415–456

Asten MW, Henstridge JD (1984) Array estimators and use of microseisms for reconnaissance of sedimentary basin. Geophysics 49:1828–1837

Bard PY (1985) Les effets de site d'origine structurale: Principaux résultats experimentaux et théoriques. In: Davidovici V (ed) Genie Parasismique. Presses de l'Ecole Nationale des Ponts et Chaussées, pp 223–238

Bard PY, SESAME-Team (2004) Guidelines for the implementation of the H/V spectral ratio technique on ambient vibrations-measurements, processing and interpretations, SESAME European research project EVG1-CT-2000-00026, deliverable D23.12, available at http://sesame-fp5.obs.ujf-grenoble.fr

Beamish D, Travassos JM (1992) The use of the D+ solution in magnetotelluric interpretation. J Appl Geophys 29:1–19

Benjumea B, Gabàs A, Bellmunt F, Macau A, Figueras S and Vilà M (2011) Geophysical techniques improving geological mapping in urban areas at two different scales. EAGE-Near Surface 2011. Oral presentation

Benjumea B, Macau A, Gabàs A, Bellmunt F, Figueras S, Cirés J (2011b) Integrated geophysical profiles and H/V microtremor measurements for subsoil characterization. Near Surf Geophy 9(5):413–425

Bonnefoy-Claudet S (2004) Nature du bruit de fond sismique: implications pour les études des effects de site, PhD. Thesis, Joseph Fourier University (Grenioble-France)

Bosch M (1999) Lithologic tomography: from plural geophysical data to lithology estimation. J Geophys Res 104:749–766

Bosch M, Zamora M, Utama W (2002) Lithology discrimination from physical rock properties. Geophysics 67(2):573–581

Cadet H, Macau A, Benjumea B, Bellmunt F, Figueras S (2011) From ambient noise recordings to site effect assessment: the case study of Barcelona microzonation. Soil Dyn Earthq Eng 31:271–281

Campanyà J, Ledo J, Queralt P, Marcuello A, Liesa M, Muñoz JA (2012) New geoelectrical characterization of a continental collision zone in the West-Central Pyrenees: constraints from long period and broadband magnetotellurics. Earth Planet Sci Lett 333–334(2012):112–121

Colombo D, Heho T, McNeice GS (2012) Integrated seismic-electromagnetic workflow for sub-basalt exploration in northwest Saudi Arabia. The Leading Edge 31,42; doi:10.1190/1.3679327.

Delgado J, López Casado C, Estévez A, Giner J, Cuenca A, Molina S (2000a) Mapping soft soils in the Segura river valley (SE Spain): a case study of microtremors as an exploration tool. J Appl Geophys 45:19–32

Delgado J, López Casado C, Giner J, Estévez A, Cuenca A, Molina S (2000b) Microtremors as a geophysical exploration tool: applications and limitations. Pure Appl Geophys 157:1445–1462

Donville B (1976) Géologie néogene de la Catalogne oriental. Bull BRGM IV 3:177–210

Fäh D, Kinf F, Giardini D (2001) A theoretical investigation of average H/V ratios. Geophys J Int 145:535–549. doi:10.1046/j.1365-246X.2001.01406.x

Falgàs E, Ledo J, Benjumea B, Queralt P, Marcuello A, Teixidó T, Martí A (2011) Integrating hydrogeological and geophysical methods for the characterization of a deltaic aquifer system. Surv Geophys. doi:10.1007/s10712-011-9126-2

Ferrer J (1971) El Paleoceno y Eoceno del borde sur-oriental de la Depresión del Ebro. Mémories suisses de Paléontologie 90:1–70

Gabàs A, Marcuello A (2003) The relative influence of different types of magnetotelluric data on joint inversions. Earth Planets Space 55(5):243–248

Gallardo LA, Meju MA (2003) Characterization of heterogeneous near-surface materials by joint 2D inversion of dc resistivity and seismic data. Geophys Res Lett 30(13):1658. doi:10.1029/2003GL017370

Gallardo LA, Meju MA (2004) Joint two-dimensional DC resistivity and seismic travel time inversion with cross-gradient constraints. J Geophys Res 109(B3):B03311. doi:10.1029/2033JB002716

Gallardo LA, Meju MA (2007) Joint two-dimensional cross-gradient imaging for magnetotelluric and seismic travel time data for structural and lithological classification. Geophys J Int 169:1261–1272. doi:10.111/j.1365-246X.2007.03366.x

Geometrics (2000) Operation manual for Stratagem system running IMAGEM, ver. 2.16: Geometrics, San José, California

Grandjean G, Gourry JC, Sanchez O, Bitri A, Garambois S (2011) Structural study of the Ballandaz landslide (French Alps) using geophysical imagery. J Appl Geophys 75:531–542. doi:10.1016/j.jappgeo.2011.07.008

Groom RW, Bailey RC (1989) Decomposition of magnetotelluric impedance tensor in the presence of local three-dimensional galvanic distortion. J Geophys Res 94:1913–1925

Guéguen P, Cornou C, Garambois S, Banton J (2007) On the limitation of the H/V spectral ratio using seismic noise as an exploration tool. Application to the Grenoble basin (France), a small apex ratio basin. Pure Appl Geophys 164:115–134

Günther T, Rücker C (2009) A new joint inversion approach applied to the combined Tomography of dc resistivity and seismic refraction data. Near Surface 2009—15th European Meeting of Environmental and Engineering Geophysics. Dublin

Ibs-Von Seht M, Wohlenberg J (1999) Microtremor measurements used to map thickness of soft sediments. Bull Seismol Soc Am 89:250–259

IGC (2003–2009), Mapa geològic de Catalunya 1:25000 (sheet 332 2-1) http://www.igc.cat

Keller GV (1987) Rock and mineral properties, in Electromagnetic methods in applied geophysics. In: Nabighian MN (ed) Society of Exploration Geophysicists, Tulsa, Oklahoma 1:13–51

Kim JH, Yi MJ, Hwang SH, Song Y, Cho SJ, Synn J-H (2007) Integrated geophysical surveys for the safety evaluation of a ground subsidence zone in a small city. J Geophys Eng 4:332–347. doi:10.1088/1742-2132/4/3/S12

Konno K, Ohmachi T (1998) Ground motion characteristics estimated from spectral ratio between horizontal and vertical components of microtremor. Bull Seismol Soc Am 88:228–241

Kühn D, Dahm T, Ohrnberber M, Vollmer D (2010) Imaging a shallow salt diaper using ambient seismic vibration beneath the densely built-up city area of Hamburg, Northern Germany. J Seism 15(3):507–531

Kwon HS, Song Y, Yi MJ, Chung HJ, Kim KS (2006) Case histories of electrical resistivity and controlled-source magnetotelluric surveys for the site investigation of tunnel construction. J Environ Eng Geophys 11:237–248

Lachet C, Bard PY (1994) Numerical and theoretical investigations on the possibilities and limitations of the Nakamura's technique. J Phys Earth 42:377–397

Ledo J, Jones AG, Siniscalchi A, Campanyà J, Kiyan D, Romano G, Rouai M and opoMed MT Team (2011) Electrical signature of modern and ancient tectonic process in the crust of the Atlas mountains of Morocco. Phys Earth Planet Interiors 185:82–88

Lee W, Stewart S (1981) Principles and applications of mirco earthquake networks. Academic Press

Macau A, Figueras S, Benjumea B, Martí A, Bellmunt F, Gabàs A (2012) Seismic microzonation for the City of Girona. Oral presentation to 7ª Asamblea Hispano-Portuguesa de Geodesia y Geofísica, Donostia

McNeice GW, Jones AG (2001) Multisite, multifrequency tensor decomposition of magnetotelluric data. Geophysics 66(1):158–173

Meric O, Garambois S, Malet JP, Cadet H, Guéguen P, Jongmans D (2007) Seismic noise based methods for soft-rocks landslides characterization. Bull Soc Geol Fr 2:137–148

Metronix (2007–2010). ADU-07(e). Operating manual. Rev. 1.3

Nakamura Y (1989) A method for dynamic characteristics estimation of subsurface using microtremors on the ground surface. Q Rep Railw Tech Res Inst 30–1:25–33

Nogoshi M, Igarashi T (1971) On the amplitude characteristics of microtremor, Part 2 (In Japanese with English abstract). J Seism Soc Jpn 24:26–40

Palacky GJ (1987) Resistivity characteristics of geologic targets, in Electromagnetic method in applied geophysics. In: Nabighian MN (ed) Society of Exploration Geophysicists, Tulsa, Oklahoma 1:53–129

Pallí L (1972) Estratigrafía del Paleógeno del Empordà y zonas limítrofes. Phd, UAB

Parolai S, Bormann P, Milkereit C (2002) New relationships between Vs, thickness of sediments and resonance frequency calculated by the H/V ratio of seismic noise for the Cologne area (Germany). Bull Seismol Soc Am 92:2521–2527

Rodi W, Mackie R (2001) Nonlinear conjugate gradients algorithm for 2-D magnetotelluric inversion. Geophysics 66:174–187

Saula E, Picart J, Mató E, Llenas M, Losantos M, Berástegui X, Agustí J (1994) Evolución geodinámica de la fosa del Empordà y las Sierras Transversales. Acta Geol Hisp 29(2–4):55–75

SESARRAY http://www.geopsy.org

Solé Sabarís L (1948) Observaciones sobre el Plioceno de la comarca de La Selva (Gerona). Estud Geol 8:287–307

Vilà M, Pi R, Cirés J, de Paz A, Beràstegui X (2010) Geological assessing of urban environments with a systematic mapping survey: the 1:5000 urban geological map of Catalonia. Geophys Res Abstracts, vol. 12, EGU General Assembly

Vozoff K (1991) The magnetotelluric method, in electromagnetic method in applied geophysics: In: Nabighian MN (ed) Society of Exploration Geophysicists, Tulsa, Oklahoma 2B:641–711

Wathelet M (2003) Report on the inversion of velocity profile and version 0 of the inversion software. SESAME Report D14.07

Wathelet M, Jongmans D, Ohrnberger M (2004) Surface wave inversion using a direct search algorithm and its application to ambient vibration measurements, EGU, first general assembly. Nice, France

Wathelet M, Jongmans D, Ohrnberger M, Bonnefoy-Claudet S (2008) Array performances for ambient vibrations on a shallow structure and consequences over V_s inversion. J Seismolog 12:1–19

Zonge KL, Hugues LJ (1991) Controlled source audio-frequency magnetotellurics, in Electromagnetic methods in applied geophysics. In: Nabighian MN (ed) Society of Exploration Geophysicists, Tulsa, Oklahoma 2B:713–809